ГОРЕНИЕ И ПЛАЗМОХИМИЯ 24 (2026) 223–232
Combustion and Plasma Chemistry https:cpc-journal.kz/

МРНТИ 31.15.19 https://doi.org/10.18321/cpc24(2)223-232

Combined-Method Synthesis of $CaTiO_3$ and $SrTiO_3$ Perovskites with *n*-Hexane: Impact on Structure and Microstructure

Zh.A. Abdimomyn[1*], M.M. Mataev[1], Zh.I. Tursyn[1], A.N. Torgaeva[1], K. Ramachandran[2], A.A. Bakibayev[3]

[1]Kazakh National Women's Teacher Training University, Aiteke Bi Str., 99, Almaty, Kazakhstan
[2]SRM Institute of Science and Technology, Chennai, India
[3]Tomsk Polytechnic University, Lenin Ave., 30, Tomsk, Russia

ARTICLE INFO

Received
01.03.2026

Received in revised form
06.05.2026

Accepted
12.05.2026

Keywords:
perovskite titanates; *n*-hexane; $CaTiO_3$; $SrTiO_3$; XRD; SEM; FTIR

ABSTRACT

This study reports the synthesis of $CaTiO_3$ and $SrTiO_3$ with a perovskite structure by a combined route involving preliminary wet mixing of $CaCO_3$/$SrCO_3$ carbonates and TiO_2 in *n*-hexane, followed by a solid – state reaction during high-temperature calcination. The phase composition and crystal structure of the obtained materials were examined by X-ray diffraction with Rietveld refinement, while the microstructure and elemental distribution were studied using SEM/EDX, and local structure and surface groups were probed by ATR-FTIR spectroscopy. It is shown that the presence of the organic solvent and the applied thermal treatment lead to the formation of single-phase $CaTiO_3$ and $SrTiO_3$ with orthorhombic and cubic modifications, respectively, and with crystallographic parameters with reference PDF cards. The average crystallite size calculated using the Sherrer equation confirmed the nanocrystalline nature of the powders, whereas SEM/EDX analysis reveals a highly porous microstructure and a homogeneous elemental distribution without noticeable metallic impurities. It is established that A-site cation substitution Ca^{2+}/Sr^{2+} in combination with *n*-hexane wet mixing induces systematic changes in lattice symmetry, IR band positions and agglomerate morphology, enabling targeted tuning of the texture and potential functional properties of perovskite titanates. The proposed combined approach is a technologically simple and scalable method for producing nanostructured oxide perovskites that are promising as supports and active phases in catalytic systems for combustion processes, plasma-chemical oxidation and functional ceramics.

1. Introduction

Perovskite-type oxides with the general formula ABO_3 are of particular interest in this context due to their high thermal and chemical stability, as well as their combination of electrical and catalytic properties. Calcium and strontium titanates ($CaTiO_3$ and $SrTiO_3$) are considered classical model systems for which it is relatively straightforward to describe the correlation between crystal-chemical properties and the microstructure of material [1].

Photo- and electrochemical energy conversion in $CaTiO_3$ has recently been widely studied, in particular its use as a photocatalyst for the degradation of organic pollutants. A number of studies have shown that modifications to the material structure (including doping and heterostructure formation) improve the quantum yield and shift the spectral sensitivity toward the visible region [2]. $SrTiO_3$ is also recognized as a promising material for electronics, thermoelectric technologies, automotive fuel cells, and hybrid solar cells, where it can serve an electron transport layer and a thermally stable functional compound [3].

$CaTiO_3$ exhibits orthorhombic perovskite-like deformation at room temperature and belongs to the Pbnm group due to the tilt and orientation of the octahedral structure of TiO_6 [4]. In particular, $SrTiO_3$ crystallizes in a nearly ideal cubic perovskite lattice (space group Pm-3m), where Sr^{2+} ions are localized at the junctions of the cubic sublattice of the A-site, and Ti^{4+} ions are in the center of the BO_6 octahedra. Differences in symmetry sizes and lattice distortion determine different dielectric properties, density

*Corresponding author: Zh.A. Abdimomyn; E-mail address: zhazi_0313@mail.ru

of states at band boundaries, and charge transport mechanisms. It is due to these characteristics that the material is suitable for applications in electronics, photocatalysis, and catalytic oxidation [5].

The structural stability of ABO_3 perovskites such as $CaTiO_3$ and $SrTiO_3$ is usually characterized by the Goldschmidt tolerance factor and its modern modifications, which can predict stable composition ranges and types of structural distortions [6]. The examples such as $CaTiO_3$ and $SrTiO_3$ show that the tilt angle of TiO_6 octahedra decreases when the A-site cation with a smaller radius (Ca^{2+}) is replaced by a larger one (Sr^{2+}), and the structure tends to approach the ideal cubic arrangement, accompanied by changes in the band gap and phase-transition behavior [7].

In practice, classical titanates are synthesized by various methods, mainly chemical approaches including sol-gel, polymer complexes, oxalate and hydrothermal synthesis, whereas a relatively simple and classical route is solid-state synthesis using carbonates and TiO_2 [8]. Chemical methods allow for fairly precise control over the morphology and composition of the material, but practical implementation often involves multistage solution procedures, the use of organic reagents, and complex heat-treatment regimes, which limits their scalability [9]. Solid-phase synthesis from carbonates and TiO_2 is generally simple and easy to implement, but typically requires high temperatures and long holding times to achieve a single-phase state, and the degree of homogenization of the starting mixture is also very sensitive to the properties of the solid reaction [10].

The initial mixing method for the reagents (high-energy milling, mechanochemical activation, and wet mixing in organic solvents) significantly affects the rate of the solid-phase reaction, the perovskite formation temperature, the crystallite size, and the morphology of the resulting powders.

High-energy and wet milling enhance diffusion and shift the temperature range of perovskite phase formation toward lower values. For $CaTiO_3$/$SrTiO_3$ systems, these methods are usually investigated independently of each other and under different experimental conditions [11].

A significant body of literature data supports the modification of $CaTiO_3$ and $SrTiO_3$ by doping and creating composites with g-C_3N_4, carbon materials and transition-metal oxides, which reported to improve their photocatalytic and catalytic properties. Significant efforts are needed to understand the fundamental aspects of phase formation and microstructure of pure $CaTiO_3$ and $SrTiO_3$ obtained under the same conditions. Therefore, it is crucial to conduct a proper comparison of their structural and morphological properties and introduce rational modifications in the future work of this paper [12].

Particular attention should be paid to the comparative study of the effect of a simple wet milling method in an organic solvent on the solid-phase synthesis of two titanates under the same thermal treatment. However, wet mixing of $CaTiO_3$ and $SrTiO_3$ precursors is a relatively new direction, and only a few studies have been carried out in aqueous or alcoholic media, while more complex systems have been explored using complexing agents. There are limited data on the use of non-polar solvents such as *n*-hexane to simplify process engineering while maintaining high phase purity [13].

This study focuses on calcium and strontium perovskite titanates, $CaTiO_3$ and $SrTiO_3$, obtained by solid-state methods from $CaCO_3$ and $SrCO_3$ carbonates with TiO_2 after preliminary wet grinding in *n*-hexane. The paper presents a simple and reproducible process for them synthesis of $CaTiO_3$ and $SrTiO_3$ under identical thermal treatments and compares of the phase composition, microstructure and IR spectra of the developed perovskites [14]. The scientific novelty of this work lies in the systematic comparison of the phase-formation processes and structural-morphological features of $CaTiO_3$ and $SrTiO_3$ synthesized under identical solid-state calcination conditions with preliminary grinding in a simple organic solvent. This approach facilitates the analysis of the role of the A-site cation and of homogenization conditions during the formation of single-phase perovskite structures [15]. The relevance of this work is determined by the fact that the obtained data provide a basis for further studies of perovskite titanates as supports and active phases in high-temperature catalytic oxidation, photocatalysis and combustion processes, where heat-resistant materials with controlled microstructure and high chemical stability are required. Perovskite-type oxides with the general formula ABO_3 are widely employed as heterogeneous catalysts owing to their compositional flexibility, high thermal stability and tunable redox properties, as highlighted in numerous recent reviews on perovskite-based catalytic systems. In particular, such materials have demonstrated excellent performance in key processes, including the dry reforming of methane and the total oxidation of hydrocarbons [3].

Although the present study is primarily devoted to the synthesis and structural-morphological

characterization of $CaTiO_3$ and $SrTiO_3$ powders, these materials are known as promising catalysts and photocatalysts for various oxidation and reduction reactions. Numerous studies report that perovskite titanates exhibit appreciable activity in photocatalytic degradation of organic pollutants and in oxidation of small molecules, which makes the obtained powders potentially attractive for such applications. A detailed evaluation of their photocatalytic performance will be the subject of future work.

2. Experimental

2.1. Materials and Methods

Calcium carbonate ($CaCO_3$), strontium carbonate ($SrCO_3$) and titanium dioxide (TiO_2, rutile) were selected as starting reagents. Chemically pure $CaCO_3$ («Reakhim») was used as calcium carbonate, titanium dioxide TiO_2 (IV) (chemically pure) was obtained from the same manufacturer («Reakhim»). High-purity strontium carbonate, $SrCO_3$, (grade 7-2) was supplied by Krasny Khimik, Russia. The carbonate and TiO_2 powders were weighed in a stoichiometric ratio relative to the ABO_3 composition, in which the ratio of the A-position cation (Ca^{2+} or Sr^{2+}) to Ti^{4+} molar ratio equal to 1:1.

Homogenization was carried out using n-hexane as a dispersion medium. The suspension was prepared by mixing the powder components in a specified ratio, adding n-hexane, and milling the mixture in a ball mill with stainless-steel balls for 40 min, which ensured a high degree of contact and homogenization and reduced the particle size due to impact and friction [16]. In the combined route, *n*-hexane thus serves as a non-polar dispersion medium to promote wet mixing of the starting powders and to improve the homogeneity of the precursor mixture prior to calcination. The use of a liquid medium facilitates more intimate contact between the reactants compared to simple dry mixing and is expected to affect both phase formation and the resulting particle morphology.

After evaporation of *n*-hexane, the dried mixture was heated in two stages in a corundum crucible in air. The initial calcination step involved heating the material to 900 ºC at a rate of 3-5 ºC/min and holding for 2 h to decompose the carbonates and activate solid-state interactions [17]. The product was then cooled in the furnace and ground in an agate mortar to obtain a homogeneous powder, which was subjected to further treatment. In the second calcination step, the material was heated to 1350 ºC with a gradually increasing temperature and held for 6 h to form and crystallize the perovskite phase, after which it was cooled in the furnace to room temperature. [18].

2.2. Characterization Methods

The crystal structures of the synthesized calcium and strontium titanate samples were studied using X-ray diffraction (XRD). At room temperature, the diffraction patterns of the crystals were measured on a Miniflex 600 diffractometer (Rigaku) using Cu Kα radiation (U = 30 kV, I = 10 mA) at a count rate of 1000 counts/s and a time constant of 5 s. The data were collected in the 2θ range from 5º to 90º . Phase analysis and Rietveld refinement were carried out using the PDF-5+ database.

The IR spectra of the $CaTiO_3$ and $SrTiO_3$ samples were obtained using Fourier transform infrared spectroscopy (FTIR-ATR) on a Bruker spectrometer (Application Note Team, Germany) in the spectral range of 4000-400 cm^{-1}. Powder samples directly pressed onto the ATR crystal were used to acquire the spectra. The spectra were processed using the standard (Bruker OPUS) with baseline correction and intensity normalization.

The morphology and microstructure were examined using a Thermo Scientific™ Axia™ ChemiSEM™ scanning electron microscope at an accelerating voltage of 20 kV, a working distance of approximately ~11 mm, and various magnifications. A Bruker scanning electron microscope (SEM) (Application Note Team, Germany) was used to obtain elemental distribution maps, perform qualitative and quantitative analysis, and determine the elemental contents in the samples.

3. Results and Discussion

The experimental X-ray diffraction patterns of the synthesized $CaTiO_3$ and $SrTiO_3$ samples are shown in Fig. 1a and 1b in comparison with the reference data from the ICDD database. The positions of all observed maxima are in excellent agreement with the reflections of the corresponding perovskite phases (PDF №01-077-8906 for $CaTiO_3$ and PDF №01-090-6518) for $SrTiO_3$.

In the case of the $CaTiO_3$ sample, the Rietveld refinement of the powder diffraction pattern using the PDF reference card 01-077-8906 shows that the compound crystallizes in an orthorhombic perovskite-type structure (ANX class ABX_3, space

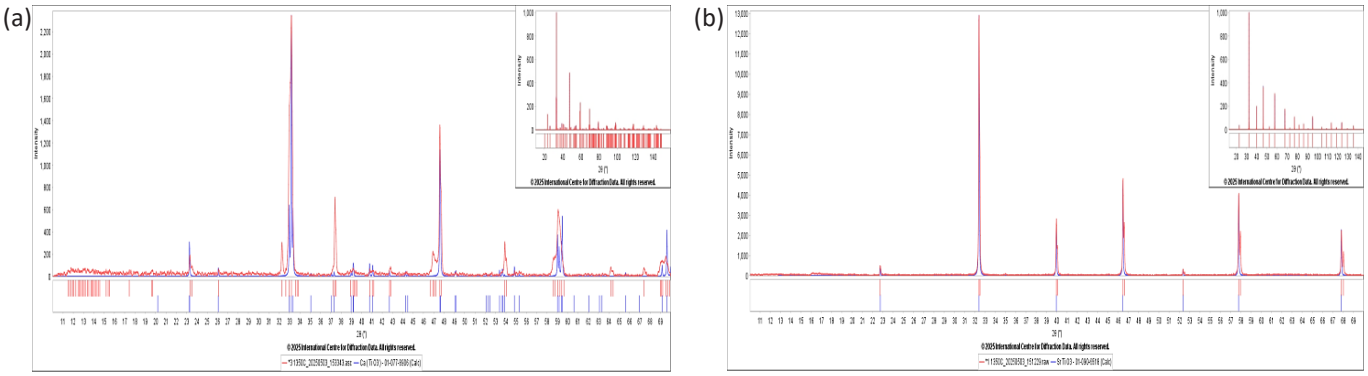

Fig. 1. Experimental X-ray diffraction patterns of the synthesized samples and reflection points from the ICDD data (a) $CaTiO_3$, (b) $SrTiO_3$. The Rietveld refinement of the XRD profile is shown in the insets.

group P_{bnm}, centrosymmetric). For this phase, the crystallographic parameters are as follows: lattice parameters a = 5.3709 Å, b = 5.4280 Å, c = 7.6268 Å, unit cell volume V = 222.35 Å^3, number of formula units Z = 4, and calculated density ρ = 4.06 g/cm^3, as listed in Table X. The low value of the total R-factor (R = 0.01) and the absence of systematic features in the difference curve indicate a high quality of the fit and support the correctness of the structural model used.

Rietveld analysis of the $SrTiO_3$ sample, based on the PDF reference card 01-090-6518, confirms the formation of a cubic perovskite phase (ANX class ABX_3, space group Pm-3m, centrosymmetric structure). All observed reflections are fully indexed in a cubic unit cell with lattice parameters a = b = c = 3.9052 Å and unit cell volume V = 59.58 Å^3 at Z = 1, in agreement with the reference data for strontium titanate (tausonite). The calculated density ρ is 5.11 g/cm^3. The total R-factor of 0.275 corresponds to an acceptable, though less perfect, agreement, with some residual deviations at higher 2θ angles, which is sufficient for reliable phase identification and confirmation of the perovskite structure.

It is therefore reasonable to conclude that both samples crystallize in oxide perovskite structures of the ABX_3 type, where Ca^{2+}/Sr^{2+} cations occupy the A sites, Ti^{4+} occupies the B sites and oxygen forms the X sublattice, in accordance with the ANX information from the PDF cards and the overall stoichiometry of the compositions.

The average crystallite size was estimated using the Debye-Scherrer equation, which relates the crystallite size to the broadening of X-ray diffraction peaks. The Scherrer formula used in this calculation is:

$$D = \frac{\kappa\lambda}{\beta\cos\theta}$$

where: D – is the average crystallite size (also called the «crystallite size»); k – is a dimensionless coefficient in the calculations (usually taken to be 0.9); λ – X-ray wavelength; β – i-s the full width of the diffraction peak (also known as the «width») in radians; θ – is the diffraction angle.

Based on the broadening of the diffraction peaks, the average crystallite size D was estimated using the Scherrer formula, and the results are summarized in Table 1. The obtained values are significantly smaller than the particle sizes determined from the SEM data, indicating the agglomeration of several nanocrystallites into micrometer-sized particles.

Table 1. Crystallographic parameters of $CaTiO_3$ and $SrTiO_3$ perovskites obtained by X-ray structural analysis

Sample	$CaTiO_3$	$SrTiO_3$
Space group	Pbnm	Pm-3m
Lattice parameters (Å)		
a (Å)	5.3709 Å	3.9052 Å
b (Å)	5.4280 Å	3.9052 Å
c (Å)	7.6268 Å	3.9052 Å
Unit cell volume,V (Å^3)	222.35	59.58
Calculated density, ρ (g/cm^3)	4.061	5.11
Z	4	1
R-factor	0.01	0.275
DScherrer , nm	20 nm	41 nm

The IR spectra of $CaTiO_3$ and $SrTiO_3$ samples obtained at 1350 °C were analyzed using the ATR method in the range from 400 to 4000 cm^{-1}. The IR spectrum of $CaTiO_3$ powder is shown in Fig. 2a.

An intense band is observed in the low-frequency region of 400-800 cm^{-1} at 638 cm^{-1} for the $CaTiO_3$ sample (Fig. 2a), which can be attributed to the stretching vibrations of Ti–O bonds in TiO_6 octahedra, typical of the $CaTiO_3$ perovskite lattice. The bands at 769 and 869 cm^{-1} are assigned to O–Ti–O bending

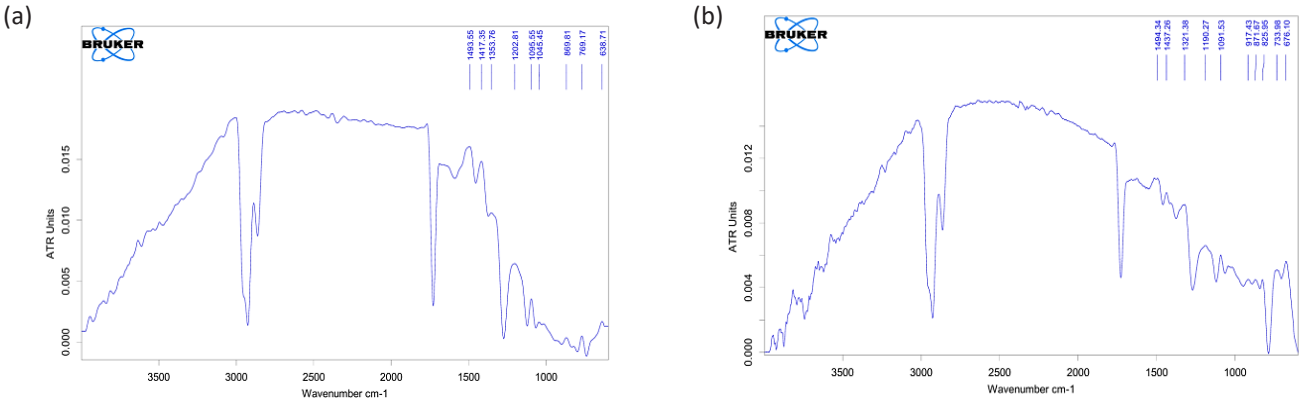

Fig. 2. IR spectra of $CaTiO_3$ and $SrTiO_3$ samples obtained at 1350 ºC (a) $CaTiO_3$, (b) $SrTiO_3$.

vibrations and the splitting of vibrational modes caused by the orthorhombic distrotion of the structure. The bands in the region of 1045, 1095 and 1202 cm^{-1} are associated with asymmetric stretching vibrations of carbonate groups $\nu_3(CO_3^{2-})$ due to the surface adsorption of CO_2. Weak bands in the region of about 1630-1650 cm^{-1} and a broad band near 3400-3450 cm^{-1} are related to bending and stretching vibrations of H–O–H and O–H in adsorbed water and hydroxyl groups. The absence of significant bands in the range of 850-950 cm^{-1} indicates the absence of detectable unreacted TiO_2.

The FTIR spectrum of $SrTiO_3$ (Fig. 2b) is characterized by bands in the range of 733-767 cm^{-1}, which correspond to Ti–O stretching vibrations in TiO_6 octahedra of the cubic perovskite lattice of $SrTiO_3$. The bands at 825 and 917 cm^{-1} are attributed to Ti–O–Ti bending vibrations. A band characteristic of Ti–O and surface hydroxyl groups vibrations is observed in the range from 1091 and 1190 cm^{-1}. Bands at 1321, 1473 and 1494 cm^{-1} correspond to $\nu_3(CO_3^{2-})$ carbonate groups formed as a result of CO_2 adsorption on the particle surface. The absence of characteristic $SrCO_3$ and SrO bands, confirming the absence of the corresponding impurity phases, is consistent with the results of X-ray diffraction analysis and indicates the stoichiometric formation of $SrTiO_3$ perovskite.

Scanning electron microscopy of the microstructure of $CaTiO_3$ and $SrTiO_3$ samples was performed at various magnifications. Loose agglomerates of $CaTiO_3$ (Fig. 3a, b), formed from small particles of predominantly plate-like and irregular morphology, range in size from 0.1 to 0.3 µm, while the average particle size, based on SEM images used for analysis, is estimated to be ~0.2 µm. The microstructure is characterized by pronounced porosity and the presence of inter-agglomerate voids, indicating incomplete sintering under the chosen synthesis conditions and leading to an increase the specific surface area of the material [19].

The $SrTiO_3$ samples form relatively compact aggregates (Fig. 4a, b) with nearly equiaxed grains of approximately 0.2-0.5 µm in size and an average particle size of 0.3-0.4 µm. In contrast, the microstructure of $SrTiO_3$ is denser than that of $CaTiO_3$, with a smaller proportion of large pores and distinct grain boundaries; the higher degree of densification may be related to the specific features of the crystal lattice and the grain growth mechanism during high temperature calcination.

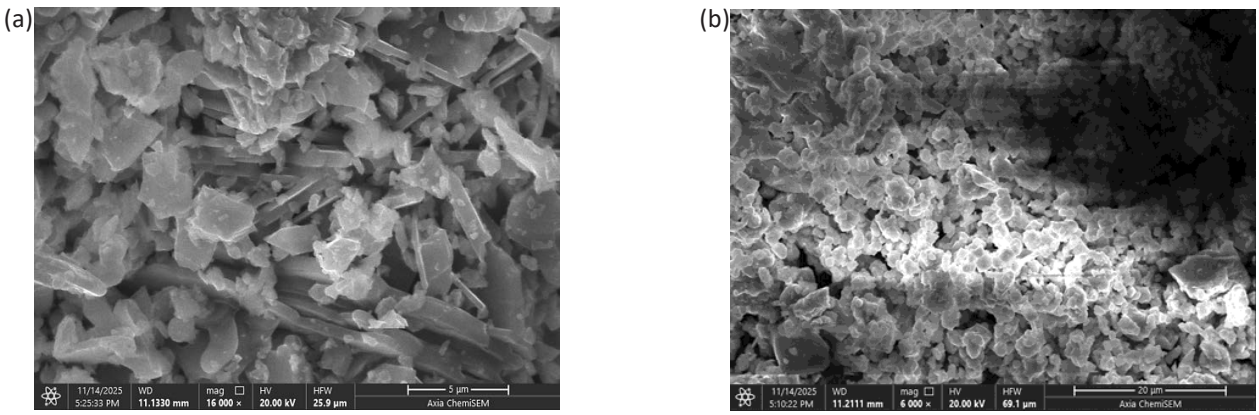

Fig. 3. SEM images of calcium titanate ($CaTiO_3$) powder obtained at various magnifications: (a), (b) general appearance of agglomerates and particle morphology.

The discrepancy between the crystallite size estimated from XRD (tens of nanometers) and the particle size observed in SEM images (hundreds of nanometers) indicates pronounced agglomeration. For applications in photocatalysis, where high external surface area and good dispersion are crucial, further optimization aimed at suppressing particle sintering (use of dispersants, milder thermal treatment, post-synthesis grinding or milling or high-energy milling) would be necessary.

Energy-dispersive X-ray (EDX) elemental mapping was performed to analyze the microstructure and the spatial distribution of oxygen, calcium, and titanium in the $CaTiO_3$ sample. No local enrichment or depletion of any of these elements was detected, indicating a uniform of distribution of cations and oxygen. Quantitative elemental analysis shows that the oxygen, calcium and titanium atoms are homogeneously distributed within agglomerates of approximately 30µ (see Fig. 5a). Similarly, for the $SrTiO_3$ sample (Fig. 5b), the EDX maps reveal a homogeneous spatial distribution of oxygen, titanium, and strontium within regions of about 40 µm (Fig. 5b). Quantitative elemental characterization of $SrTiO_3$ confirms that these elements are uniformly distributed across the probed areas. In both cases, SEM observations indicate that the powdered solids consist of aggregates built from nanometer sized primary particles, consistent with the nanocrystalline character inferred from XRD.

The elemental distribution with qualitative and quantitative analysis was determined by scanning electron microscopy. Spectral data with elemental analysis results for (a) $CaTiO_3$ and (b) $SrTiO_3$ are shown in Fig. 6.

It should be noted that the final calcination temperature of 1350 °C is energy demanding. In future work, the energy consumption can be reduced by employing precursor based routes (e.g. citrate or Pechini-like methods, sol-gel synthesis) that provide intimate mixing at the molecular level and allow perovskite phase formation at lower temperatures (typically 900-1200 °C), by introducing aliovalent dopants to enhance cation diffusion, as well as by optimizing the dwell time and heating rate during the thermal treatment.

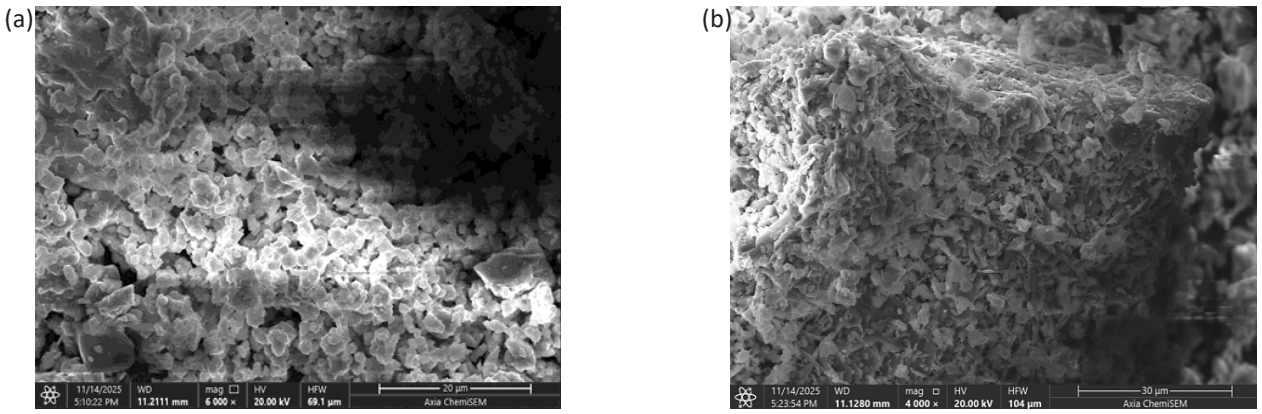

Fig. 4. SEM images of strontium titanate ($SrTiO_3$) powder at different magnifications: (a), (b) general view of agglomerates and particle morphology.

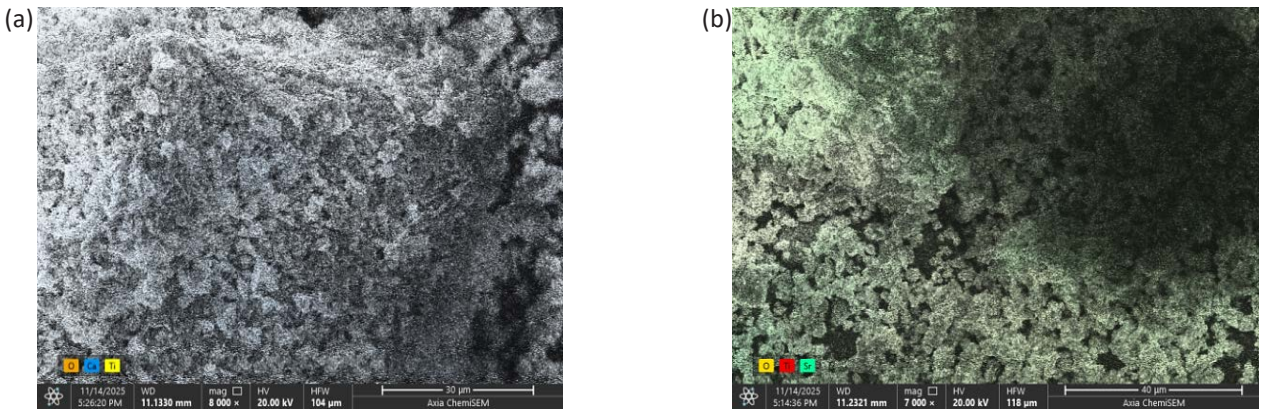

Fig. 5. (a) superimposed elemental distribution map corresponding to the $CaTiO_3$ sample (in order of distribution and color scheme of O, Ca, and Ti); (b) superimposed elemental distribution map of the $SrTiO_3$ sample (in order of distribution and color code of O, Ti, and Sr).

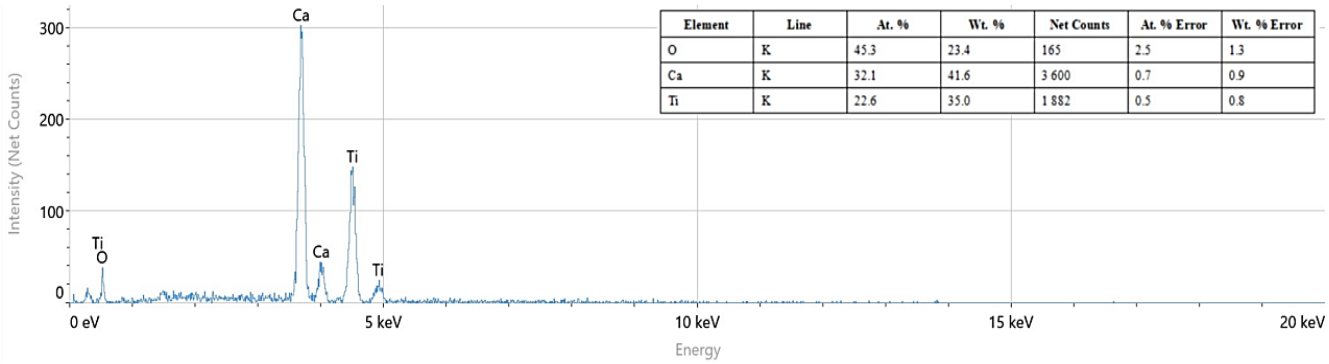

Element	Line	At. %	Wt. %	Net Counts	At. % Error	Wt. % Error
O	K	45.3	23.4	165	2.5	1.3
Ca	K	32.1	41.6	3 600	0.7	0.9
Ti	K	22.6	35.0	1 882	0.5	0.8

Fig. 6a. EDX spectrum of $CaTiO_3$ sample. Inset: integrated elemental analysis results.

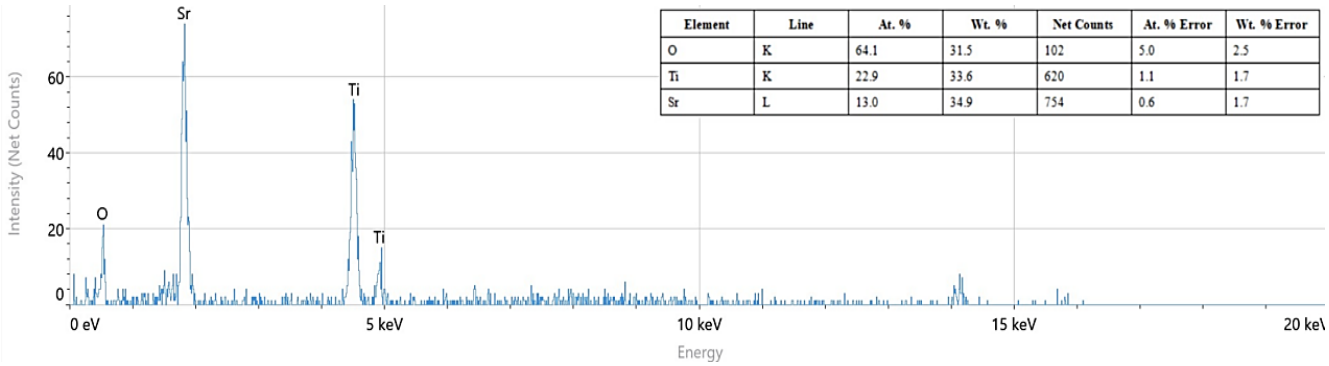

Element	Line	At. %	Wt. %	Net Counts	At. % Error	Wt. % Error
O	K	64.1	31.5	102	5.0	2.5
Ti	K	22.9	33.6	620	1.1	1.7
Sr	L	13.0	34.9	754	0.6	1.7

Fig. 6b. EDX spectrum of the $SrTiO_3$ sample. Inset: integrated elemental analysis results.

4. Conclusion

This study presents an optimal and technologically feasible solid-phase method for the synthesis of calcium and strontium perovskite titanates, where preliminary wet milling of the reactants in n-hexane allows the preparation of nanocrystalline powders with controlled crystal structures. Using the Rietveld method and X-ray diffraction analysis, it was established that a two-stage heat treatment ensures almost complete conversion of the starting carbonates and TiO_2 into single-phase perovskite products: $CaTiO_3$ crystallizes in the orthorhombic Pbnm structure, whereas $SrTiO_3$ adopts the cubic Pm-3m structure. IR spectroscopy of the materials also showed that these target phases are formed, as evidenced by characteristic Ti–O and Ti–O–Ti stretching and bending vibrations and the absence of bands attributable to residual TiO_2, SrO or $CaCO_3$.

The average crystallite size, determined using the Scherrer equation based on the XRD peak broadening, confirms that the obtained titanates are nanocrystalline, with crystallite sizes on the order of tens of nanometers, which is consistent with literature data on perovskite oxides synthesized at comparable temperatures. Scanning electron microscopy (SEM) revealed porous secondary agglomerates formed by submicron particles: $CaTiO_3$ consists primarily of plate-like particles with a looser microstructure, whereas $SrTiO_3$ is composed of a denser system of nearly equiaxed grains. Energy-dispersive X-ray analysis confirmed the homogeneity of the synthesized powders and the absence of significant amounts of foreign metallic impurities, which corroborates the XRD data indicating the single-phase nature of the samples.

A comparison of the structural, spectral and microstructural properties of $CaTiO_3$ and $SrTiO_3$ obtained by the same combined method demonstrates that substitution of the A-site cation leads to systematic changes in crystal symmetry parameters, degree of sintering and powder texture, which is fundamental for the design of perovskite compounds with tailored functional properties. The synthesized nanocrystalline porous powders with a uniform elemental distribution are promising as functional ceramics, high-temperature catalytic and sorption materials, and as model systems for studying the relationship between composition, microstructure and performance characteristics of perovskite titanates. The employment of n-hexane as a dispersion medium in the wet mixing step is expected to contribute to a more homogeneous distribution of Ca/Sr and Ti species in the precursor

mixture, which in turn may facilitate perovskite phase formation and influence particle agglomeration. A systematic comparison with other solvents and dry-mixed precursors will be addressed in future work.

Author Contributions

Zhazira Abdimomyn – Methodology, Investigation, Formal analysis, Writing – original draft. **Mukhametkali Mataev** – Resources, Supervision, Writing – review & editing. **Zhanar Tursyn** – Conceptualization, Visualization. **Arailym Torgaeva** – Writing – review & editing, Translation. **K. Ramachandran** – Validation, Data curation. **Abdigali Bakibayev** – Supervision, Resources.

Conflict of Interest Declaration

The authors declare no conflicts of interest.

Acknowledgments

This article was prepared with the financial support of the Ministry of Education and Science of the Republic of Kazakhstan №AP26198947 «Synthesis and study of the properties of multicomponent perovskites for the development of magnetically sensitive media with controlled physicochemical characteristics», 2025-2027.

References:

[1]. M. Dawber, K.M. Rabe, J.F. Scott. Physics of $SrTiO_3$-based ferroelectrics oxides. Reviews of Modern Physics 77 (2005) 1083-1130. https://doi.org/10.1103/RevModPhys.77.1083.

[2]. C.J. Bartel, C. Sutton, B.R. Goldsmith, R. Ouyang, C.B. Musgrave, et al. New tolerance factor to predict the stability of perovskite oxides and halides. Science Advances 5 (2019) eaav0693. https://doi.org/10.1126/sciadv.aav0693.

[3]. L. Cerón-Urbano, J. Aguilar, J.E. Diosa, E. Mosquera-Vargas. Nanoparticles of the perovskite-structure $CaTiO_3$ system: The synthesis, characterization, and evaluation of its photocatalytic capacity to degrade emerging pollutants, Nanomaterials 13 (2023) 2967. https://doi.org/10.3390/nano13222967.

[4]. M.V. Zdorovets, D.B. Borgekov, I.Z. Zhumatayeva, I.E. Kenzhina, A.L. Kozlovskiy. Synthesis, properties and photocatalytic activity of $CaTiO_3$ - based ceramics doped with lanthanum. Nanomaterials 12 (2022) 2241. https://doi.org/10.3390/nano12132241.

[5]. A. Kumar, C. Schuerings, S. Kumar, A. Kumar, V. Krishnan. Perovskite-structured $CaTiO_3$ coupled with g - C_3N_4 as a heterojunction photocatalyst for organic pollutant degradation, Beilstein Journal of Nanotechnology 9 (2018) 671-685. https://doi.org/10.3762/bjnano.9.62.

[6]. F. Yang, M. Li, L. Li, P. Wu, E. Pradal-Velázquez, et al. Defect chemistry and electrical properties of sodium bismuth perovskite. Journal of Materials Chemistry A 6 (2018) 5243-5254. https://doi.org/10.1039/C7TA09245H.

[7]. A. Tarancon, M. Burriel, J. Santiso, S.J. Skinner, J.A. Kilner. Advances in layered oxide cathodes for intermediate temperature solid oxidefuelcells. Journal of Materials Chemistry 20 (2010) 3799-3813. https://doi.org/10.1039/B922430K.

[8]. R. Ali, M. Yashima. Space group and crystal structure of the perovskite $CaTiO_3$ from 296 to 1720 K. Journal of Solid State Chemistry 178 (2005) 2867-2872. https://doi.org/10.1016/j.jssc.2005.06.027.

[9]. H. Zhang, M.M. Schmitt, L. Bastogne, X. He, P. Ghoses. Finite-temperature properties and the hidden ferroelectric phase of bulk $CaTiO_3$ from second principles. arXiv preprint: 2505.03129v3. (2025). https://arxiv.org/pdf/2505.03129.

[10]. S.A.U. Portia, S. Rajkumar, E. Elanthamilan, J.P. Merlin, K. Ramamoorthy. Effect of annealing temperature on structural, optical and visible light photocatalytic performance of $CaTiO_3$ catalysts synthesized by simple sol-gel technique. Inorganic Chemistry Communications 119 (2020) 108051. https://doi.org/10.1016/j.inoche.2020.108051.

[11]. J.F. Reynes, F. Leon, F. Garcia. Mechanochemistry for organic and inorganic synthesis. ASC Organic & Inorganic Au 4 (5) (2024) 432-470. https://doi.org/10.1021/acsorginorgau.4c00001.

[12]. E. Rocha-Rangel, W.J. Pech-Rodríguez, J.L. Hernández, C.A. Calles-Arriaga, E.N. Armendariz-Mireles, et al. Synthesis of $SrTiO_3$ by the calcination of $SrCO_3$ and TiO_2 mixtures intensively ground by means of high energy milling. Archives of Metallurgy and Materials 65 (2) (2020) 621-626. https://doi.org/10.24425/amm.2020.132801.

[13]. A.A. Bayode, O.T. Ore, E.A. Nnamani, B. Sotunde, D.T. Koko, et al. Perovskite oxides: Syntheses and perspectives on their application for nitrate reduction. ACS Omega 9 (2024) 19770-19785. https://doi.org/10.1021/acsomega.4c01487.

[14]. P. Dulian. Solid-state mechanochemical syntheses of perovskites, Chapter 2 - Perovskite Materials

Synthesis, Characterisation, Properties and Applications. IntechOpen London (2016) 3-26. https://doi.org/10.5772/61521.

[15]. M. Foroughipour, A. Nezamedeh-Ejhieh. $CaTiO_3$/g-C_3N_4 heterojunction-based composite photocatalyst: Part I: Experimental design, kinetics, and scavenging agents' effects in photocatalytic degradation of gemifloxacin. Chemosphere 334 (2023) 139019. https://doi.org/10.1016/j.chemosphere.2023.139019.

[16]. D. Anand, K. Ramachandran, M. Silambarasan, J. Gajendiran, S. Gajendran, et al. Various concentrations of yttrium oxide (Y_2O_3) doping induce changes in structural, magnetic, optical, and photoluminescence properties of solid-state synthesized strontium titanate ($SrTiO_3$) compounds for optoelectronic device applications. Optical Materials 147 (2024) 114706. https://doi.org/10.1016/j.optmat.2023.114706.

[17]. D. Wu. Synthesis of $SrTiO_3$ nanoparticles for photocatalytic applications. Highlights in Science, Engineering and Technology 116 (2024) 9-20. https://doi.org/10.54097/hay5w567.

[18]. P. Kaur, R. Arora, S.K. Shahi, J.S. Shahi. Green Synthesis of Nano-sized Calcium Titanate $CaTiO_3$ Using Solid State Mechano-Chemical Solventless Method and its Characterization. International Journal for Research in Engineering Application & Management 4 (2018) 3751-3756. https://www.ijream.org/papers/IJREAMV04I013751.pdf.

[19]. S.J. Jiao, J.L. Yan, G.P. Sun, Y. Zhao. Electronic structures and optical properties of Nb-doped $SrTiO_3$ from first principles. Journal of Semiconductors 37 (2016) 072001. http://dx.doi.org/10.1088/1674-4926/37/7/072001.

About the Authors

Zh.A. Abdimomyn – PhD student, Kazakh National Women's Pedagogical University, Almaty, Kazakhstan
E-mail: zhazi_0313@mail.ru

M.M. Matayev – Doctor of Chemical Sciences, Professor, Kazakh National Women's Pedagogical University, Almaty, Kazakhstan
E-mail: mataev_06@mail.ru
ORCID: https://orcid.org/0000-0002-9057-5443

Zh.I. Tursyn – PhD, Senior Lecturer, Kazakh National Women's Pedagogical University, Almaty, Kazakhstan
E-mail: zhanar.tursin@mail.ru
ORCID: https://orcid.org/0000-0002-0349-4953

A.N. Torgaeva – Master's Student, Kazakh National Women's Pedagogical University, Almaty, Kazakhstan
E-mail: arailymtorgayeva@gmail.com

K. Ramachandran – Associate Professor, Department of Physics, SRM Institute of Science and Technology, Chennai, India
E-mail: ramachak1@srmist.edu.in
ORCID: https://orcid.org/0000-0002-0977-186X

A.A. Bakibaev – Doctor of Chemical Sciences, Professor, Tomsk Polytechnic University, Tomsk, Russia
E-mail: bakibaev@mail.ru

Комбинированный синтез перовскитов $CaTiO_3$ и $SrTiO_3$ в присутствии *н*-гексана: влияние на формирование структуры и микроструктуры

Ж.А. Әбдімомын[1*], М.М. Матаев[1], Ж.И. Тұрсын[1], А.Н. Торғаева[1], К. Рамачандран[2], А.А. Бакибаев[3]

[1]Казахский национальный женский педагогический университет, ул. Айтеке би, 99, Алматы, Казахстан
[2]SRM Институт науки и технологий, Ченнаи, Индия
[3]Томский политехнический университет, пр. Ленина, 30, Томск, Россия

АННОТАЦИЯ

В данной работе синтезированы $CaTiO_3$ и $SrTiO_3$ комбинированным методом с перовскитной структурой предварительным мокрым смешиванием карбонатов $CaCO_3$/$SrCO_3$ и диоксида титана TiO_2 в *н*-гексане с последующей твердофазной реакцией при высокотемпературном отжиге. Фазовый состав и кристаллическая структура полученных материалов изучены методом рентгеновской дифрактометрии с Ритвельд – уточнением, микроструктура и элементное распределение с использованием SEM/EDX, а локальная структура и поверхностные группы методом ATR–FTIR-спектроскопии. Показано, что присутствие органического растворителя и термообработка обеспечивают формирование однофазных $CaTiO_3$ и $SrTiO_3$ с орторомбической и кубической модификациями и кристаллографическими параметрами, согласующимися с эталонными PDF-картами. Расчет среднего размера кристаллитов по уравнению Шеррера подтверждает нанокристаллический характер полученных порошков, SEM/EDX-анализ выявляет развитую пористую микроструктуру и однородный элементный состав без заметных металлических примесей. Установлено, что замещение А-катиона Ca^{2+}/Sr^{2+} с использованием н-гексана на стадии мокрого смешивания приводит к систематическим изменениям в симметрии решетки, положении полос в ИК-спектрах и морфологии агломератов, что позволяет целенаправленно варьировать текстуру и потенциальные функциональные свойства перовскитных титанатов. Предложенный комбинированный подход является технологически простым и масштабируемым методом получения наноструктурированных оксидных перовскитов, перспективных в качестве носителей и активной фазы в каталитических системах для процессов горения, плазмохимического окисления и функциональной керамики.

Ключевые слова: перовскитные титанаты, *н*-гексан, $CaTiO_3$, $SrTiO_3$, XRD, SEM, FTIR

$CaTiO_3$ және $SrTiO_3$ перовскиттерін *н*-гексан қатысындағы біріктірілген әдіспен синтездеу: құрылымы мен микроструктурасының түзілуіне әсері

Ж.А. Әбдімомын[1*], М.М. Матаев[1], Ж.И. Тұрсын[1], А.Н. Торғаева[1], К. Рамачандран[2], А.А. Бакибаев[3]

[1]Қазақ ұлттық қыздар педагогикалық университеті, Айтеке би к., 99, Алматы, Қазақстан
[2]SRM Ғылым және технологиялар институты, Ченнай, Үндістан
[3]Томск политехникалық университеті, Ленин даң., 30, Томск, Ресей

АННОТАЦИЯ

Осы жұмыста $CaCO_3$/$SrCO_3$ карбонаттары мен титан диоксиді TiO_2-ні н-гексан ортасында алдын ала ылғалды араластыру арқылы перовскит құрылымы бар $CaTiO_3$ және $SrTiO_3$ материалдары синтезделді, одан кейін жоғары температурада қыздыру кезінде қатты фазалық реакция жүргізілді. Алынған материалдардың фазалық құрамы мен кристалдық құрылымы Ритвельд түзетуімен рентгендік дифрактометрия әдісімен зерттелді, микроқұрылымы мен элементтік таралуы SEM/EDX арқылы, ал жергілікті құрылымы мен беттік топтары ATR–FTIR спектроскопиясымен зерттелді.Органикалық еріткіштің пайдаланылуы және сатылы термиялық өңдеу нәтижесінде орторомбтық және кубтық модификацияларына сәйкес келетін кристаллографиялық параметрлері бар бір фазалы $CaTiO_3$ және $SrTiO_3$ перовскиттерінің түзілуі қамтамасыз етілетіні көрсетілді. Шеррер теңдеуі бойынша орташа кристаллит өлшемін есептеу алынған ұнтақтардың нанокристалдық сипатын растайды, ал SEM/EDX талдауы дамыған кеуектілігі бар микроқұрылымды және металлдық қоспаларсыз біртекті элементтік құрамды көрсетті. *Н*-гексан қатысуымен жүзеге асырылатын ылғалды араластыру кезеңінде А-катионды Ca^{2+}/Sr^{2+} алмастыру тор симметриясының, ИК-спектрлердегі жолақтардың орналасуының және агрегаттар морфологиясының жүйелі өзгерістеріне әкелетіні анықталды, бұл перовскиттік титанатардың текстурасы мен ықтимал функционалдық қасиеттерін мақсатты түрде реттеуге мүмкіндік береді. Ұсынылған біріктірілген тәсіл технологиялық тұрғыдан қарапайым және масштабталатын, наноқұрылымды перовскиттік оксидтерді алу әдісі болып табылады, олар функционалдық керамикада, каталитикалық және плазмохимиялық тотығу процестерінде қолдануға перспективалы материалдар ретінде қарастырылады.

Түйін сөздер: перовскит титанаттары, *н*-гексан, $CaTiO_3$, $SrTiO_3$, XRD, SEM, FTIR